

# Prediction-Free Coordinated Dispatch of Microgrid: A Data-Driven Online Optimization Approach

Kaidi Huang, *Student Member, IEEE*, Lin Cheng, *Senior Member, IEEE*, Ning Qi, *Member, IEEE*,  
David Wenzhong Gao, *Fellow, IEEE*, Asad Mujeeb, *Student Member, IEEE*, Qinglai Guo, *Fellow, IEEE*

**Abstract**—Traditional prediction-dependent dispatch methods can face challenges when renewables and prices predictions are unreliable in microgrid. Instead, this paper proposes a novel prediction-free two-stage coordinated dispatch approach in microgrid. Empirical learning is conducted during the offline stage, where we calculate the offline optimal state of charge (SOC) sequences for generic energy storage under different historical scenarios. During the online stage, we synthesize a dynamically updated reference for SOC and a dynamic opportunity price (DOP) based on empirical learning and real-time observations. They provide a global vision for online operation and effectively address the myopic tendencies inherent to online decision-making. The real-time control action, generated from online optimization algorithm, aims to minimize the operational costs while tracking the reference and considering DOP. Additionally, we develop an adaptive virtual-queue-based online optimization algorithm based on online convex optimization (OCO) framework. We provide theoretical proof that the proposed algorithm outperforms the existing OCO algorithms and achieves sublinear dynamic regret bound and sublinear strict constraint violation bound. Simulation-based studies demonstrate that, compared with model predictive control-based methods, it reduces operational costs and voltage violation rate by 5% and 9%, respectively.

**Index Terms**—Microgrid, online convex optimization, energy storage, coordinated dispatch, data-driven method.

## I. INTRODUCTION

**M**ICROGRID (MG) enables the integration and coordination of renewable energy sources (RES), energy storage (ES), distributed generator (DG), and load. Due to the diverse uncertainties from RES, load, prices, etc., the MG dispatch under diverse uncertainties is critical yet challenging.

Traditionally, the dispatch of MG is approached through prediction-based optimization strategies, which include robust optimization [1], stochastic optimization [2], and chance-constrained optimization [3]. These methods primarily address uncertainties in the day-ahead planning stage but often fail to adapt to real-time environmental changes. This limitation motivates the exploration of multi-period rolling-horizon dispatch that relies on continuously updated forecast data using advanced techniques such as model predictive control (MPC) [4], approximate dynamic programming [5], and reinforcement learning [6]. While these approaches can provide effective real-time operational solutions, the required precise predictions of RES outputs and market prices are typically unavailable or unreliable in many MG settings, as most lack the necessary meteorological measuring devices and numerical weather predictions [7]. Moreover, existing literature seldom accounts for the uncertainty of market prices, which can significantly affect operational costs due to their volatility and unpredictability. Therefore, existing

prediction-based approaches are still not effectively applicable and may result in poor economic performance, and worst, can also cause feasibility issues in some cases [8].

In response to these challenges, there has been a growing interest in developing online algorithms that minimize reliance on predictive models. These algorithms, notably Lyapunov optimization and online convex optimization (OCO), emphasize a pure online decision-making process devoid of any prior statistical assumptions. Lyapunov optimization, following a “1-lookahead” pattern, observes uncertainties first and then addresses them by solving the Lyapunov drift problem [9]. However, this method proves inapplicable in real-world market conditions where ES owners must bid without knowledge of future prices, and where the prices are cleared by the market after the bidding process. [8]. In contrast, OCO operates under a “0-lookahead” pattern, making preemptive decisions before uncertainties are observed.

OCO is inherently problem-dependent and does not adhere to a unified mathematical paradigm but focuses on improving performance metrics such as *regret* and *violation* [10]–[16]. The first metric *regret* measures the suboptimality of the OCO algorithm by quantifying the gap between the algorithm’s performance and a predetermined baseline. This metric is categorized based on the type of baseline: *dynamic regret* is measured against the global optimal solution, while *static regret* is compared to an optimal static decision [13]. The second metric *violation* specifically termed ( $V_{io}^{strict}$ ), evaluates the safety performance by quantifying cumulative constraint violations. Although some studies utilize a more lenient metric known as *soft constraint violation* ( $V_{io}^{soft}$ ), this does not accumulate violations provided they are offset by other strictly feasible decisions. It is generally accepted in the literature that an OCO algorithm is performing effectively if both its regret and constraint violation metrics exhibit sublinear trends with respect to the timeline of operation.

Due to its prediction-free and fast response nature, OCO has recently gained attention in power systems, particularly in the applications of demand-side management and ancillary services [17]–[19]. Reference [17] proposes an OCO-based algorithm for dynamically setting electricity prices to promote optimal usage and stabilize load curves. In [19], an OCO-based algorithm is developed for real-time management of building energy systems to enhance their contribution to grid ancillary services under uncertainties and limited information.

However, the application of OCO in the online operation of MG still faces two challenges: (i) The “myopic” nature of online algorithms: Although both OCO and Lyapunov optimization inherently rely on current system state information without the need for predictions, they inevitably possess “myopic”

TABLE I  
COMPARING OF THIS PAPER TO RELATED WORKS ON ONLINE CONVEX OPTIMIZATION

Reference	Constraint type	Regret benchmark	Regret bound	Constraint violation	Constraint violation bound
[10]	Time-varying	Dynamic	$O(\max(T^\delta P_x, T^{1-\delta}))$	$\text{Vio}^{\text{soft}}$	$O(T^{1-\delta/2})$
[11]	Time-invariant	Static	$O(\sqrt{T})$	$\text{Vio}^{\text{soft}}$	$O(1)$
[12]	Time-varying	Dynamic	$O(\sqrt{TP_x})$	$\text{Vio}^{\text{soft}}$	$O(\max(T^{3/4}, P_g))$
[13]	Time-invariant	Dynamic	$O(\sqrt{T(1+P_x)})$	$\text{Vio}^{\text{strict}}$	$O(\sqrt{T})$
[14]	Time-varying	Static	$O(\sqrt{T})$	$\text{Vio}^{\text{soft}}$	$O(T^{3/4})$
[15]	Time-varying	Static	$O(T^{\max\{1-a-c, c\}})$	$\text{Vio}^{\text{strict}}$	$T^{1/2-c/2}$
[16]	Time-varying	Static	$O(T^{\max(\delta, 1-\delta)})$	$\text{Vio}^{\text{strict}}$	$O(T^{1-\delta/2})$
This paper	Time-varying	Dynamic	$O(T^{1/2+\chi}\sqrt{1+P_x})$	$\text{Vio}^{\text{strict}}$	$O(\log_2(T)T^{1-\chi/2})$

$P_x$ : path-length, i.e., the accumulated variation of optimal decisions;  $P_g$ : function variation, i.e., the accumulated variation of constraints.

nature due to the lack of a comprehensive outlook. Traditional online optimization algorithms risk falling into local optima due to the inter-temporal coupling constraints of ES in MG. (ii) Performance metric: Dynamic regret and strict constraint violation are crucial metrics for evaluating the performance of MG management, especially in volatile environments. Achieving sublinear trends in both dynamic regret and strict constraint violation simultaneously under common assumptions remains an unaddressed challenge in existing research. Hence, to the best of our knowledge, no research work has yet developed an OCO-based algorithm for the dispatch of MG.

Motivated by the research gaps, this paper proposes a novel prediction-free coordinated dispatch framework that effectively addresses the “myopia” of online optimization, and develops an adaptive virtual-queue-based (VQB) OCO algorithm that is distinct in its capacity to surpass existing algorithms in managing both regret and violation metrics effectively. The main contributions of this research are:

1) **Dispatch Framework.** We propose a novel prediction-free coordinated dispatch framework tailored for MG dispatch under diverse uncertainties. This framework enhances traditional online optimization by resolving its inherent “myopia.” It does so by integrating a “reference” state of charge (SoC), dynamic opportunity price (DOP), and OCO. Empirical learning from the offline stage and real-time observations during the online stage allow for the continuous updating of the reference SoC, providing a comprehensive operational vision for generic energy storage (GES). Concurrently, DOP is recalculated regularly to reflect future price trends accurately, informing cost-effective control actions. These enhancements enable real-time control actions generated via OCO to optimize operational costs effectively in the long run. Numerical study demonstrates that, compared with traditional online optimization algorithm, the proposed method reduces operational costs by 11%.

2) **Solution Algorithm.** We propose an adaptive VQB online optimization algorithm that builds on the OCO framework. By introducing virtual queues with new update rules in decision-making and incorporating the expert tracking algorithm to adaptively update the learning rate, our algorithm outperforms the existing OCO algorithms in terms of both suboptimality and safety metrics, without influencing computational efficiency. Notably, this research marks the first instance of

achieving sublinear dynamic regret and strict constraint violation bounds for OCO with time-varying constraints, backed by theoretical proof. A comparative analysis with related works is encapsulated in Table I. Numerical study demonstrates that, compared with MPC-based method, the algorithm reduces operational costs and voltage violation rate by 5% and 9%, respectively, and increases computational efficiency by 19 times.

The remainder of the paper is organized as follows. The MG structure and its offline operation model are formulated in Section II. The data-driven, two-stage coordinated dispatch framework and the adaptive VQB online optimization algorithm for MG are developed in Section III. Numerical study based on ground-truth data is provided in Section IV. Finally, conclusions are summarized in Section V.

## II. PROBLEM FORMULATION

A typical MG consists of RES, DG, ES, flexible load, conventional load, etc, and can be connected to the main grid. Most of flexible loads, such as thermostatically controlled load and electric vehicle, have the attributes of ES, hence motivating the concept of “virtual energy storage” (VES). ES and VES can be considered under a common framework called GES to unify modeling. The model transformation from physical load to GES can be referenced in [3]. The offline operation model is given below.

Considering a daily operation horizon with a 5-minute time interval, the index of periods is  $t \in \Omega_T = \{1, 2, \dots, T\}$ . The objective function of MG operation model, as specified in equation (1a), aims to minimize the total operational costs, which encompass the incentive cost of GES detailed in (1b), the cost of grid power (1c), and the generation cost of DG (1d). Constraints (2)-(3) are the output limit and ramp constraint for DG. Constraints (4)-(5) limit the charge/discharge power of GES. Since sufficient conditions are satisfied, the complementary constraint for charging and discharging is relaxed and has been removed from model [20]. Constraint (6) defines the relationship among charge power, discharge power, SoC, and additional energy input from baseline consumption. Constraint (7) represents time-varying upper and lower bounds on SoC. The time-varying and stochastic power limit and SoC limit of GES can be obtained by data-driven methods (i.e., load decomposition and parameter identification) [21]. Chance

constraints (5) and (7) can adopt different confidence levels for different reliability preferences [22]. Constraint (8) ensures a sustainable energy state for the GES overtime. Constraints (9)-(12) are power flow for radial MG which can be modelled with the *DistFlow* model [23]. Constraint (13) restricts the reverse power flow due to its potential adverse effects on the grid.

Objective function:

$$\min \sum_{t \in \Omega_T} (C_t^{\text{GES}} + C_t^{\text{grid}} + C_t^{\text{DG}}) \quad (1a)$$

$$C_t^{\text{GES}} = \sum_{j \in \Omega_G} (c_{d,j}^{\text{GES}} P_{d,j,t}^{\text{GES}} + c_{c,j}^{\text{GES}} P_{c,j,t}^{\text{GES}}) \Delta t \quad (1b)$$

$$C_t^{\text{grid}} = \lambda_t P_t^{\text{grid}} \Delta t \quad (1c)$$

$$C_t^{\text{DG}} = \sum_{k \in \Omega_D} (a_k P_{k,t}^{\text{DG}}) \Delta t \quad (1d)$$

Constraints:  $\forall t \in \Omega_T, \forall k \in \Omega_D, \forall j \in \Omega_G, \forall m \in \Omega_B$

$$\underline{P}_k^{\text{DG}} \leq P_{k,t}^{\text{DG}} \leq \overline{P}_k^{\text{DG}} \quad (2)$$

$$-P_{k,\text{RD}}^{\text{DG}} \leq P_{k,t+1}^{\text{DG}} - P_{k,t}^{\text{DG}} \leq P_{k,\text{RU}}^{\text{DG}} \quad (3)$$

$$0 \leq P_{c,j,t}^{\text{GES}}, \quad 0 \leq P_{d,j,t}^{\text{GES}} \quad (4)$$

$$\mathbb{P}(P_{c,j,t}^{\text{GES}} \leq \overline{P}_{c,j,t}^{\text{GES}}) \geq 1 - \varepsilon, \quad \mathbb{P}(P_{d,j,t}^{\text{GES}} \leq \overline{P}_{d,j,t}^{\text{GES}}) \geq 1 - \varepsilon \quad (5)$$

$$\text{SoC}_{j,t+1} = (1 - \mathcal{E}_j) \text{SoC}_{j,t} + \eta_{c,j} P_{c,j,t}^{\text{GES}} \Delta t / E_j - P_{d,j,t}^{\text{GES}} \Delta t / (\eta_{d,j} E_j) + \pi_{j,t} \quad (6)$$

$$\mathbb{P}(\underline{\text{SoC}}_{j,t} \leq \text{SoC}_{j,t} \leq \overline{\text{SoC}}_{j,t}) \geq 1 - \varepsilon \quad (7)$$

$$\text{SoC}_{j,T} = \text{SoC}_{j,0} \quad (8)$$

$$P_{b+1,t}^{\text{PF}} = P_{b,t}^{\text{PF}} - P_{b+1,0,t}^{\text{PF}} - P_{m,t}^{\text{L}} + P_{m,t}^{\text{R}} + P_{m,t}^{\text{DG}} + P_{d,m,t}^{\text{GES}} - P_{c,m,t}^{\text{GES}}, b \in Br(m) \quad (9)$$

$$Q_{b+1,t}^{\text{PF}} = Q_{b,t}^{\text{PF}} - Q_{b+1,0,t}^{\text{PF}} - Q_{m,t}^{\text{L}} + Q_{d,m,t}^{\text{GES}} - Q_{c,m,t}^{\text{GES}}, b \in Br(m) \quad (10)$$

$$V_{m+1,t}^{\text{BUS}} = V_{m,t}^{\text{BUS}} - (R_b P_{b,t}^{\text{PF}} + X_b Q_{b,t}^{\text{PF}}) / V^{\text{B}}, b \in Br(m, m+1) \quad (11)$$

$$1 - \underline{V}^{\text{BUS}} \leq V_{m,t}^{\text{BUS}} \leq 1 + \overline{V}^{\text{BUS}} \quad (12)$$

$$0 \leq P_t^{\text{grid}} \leq \overline{P}^{\text{grid}} \quad (13)$$

where  $\Omega_G$ ,  $\Omega_D$  and  $\Omega_B$  are the sets of GES assets, DG assets and buses, respectively.  $c_{d,j}^{\text{GES}}$ ,  $c_{c,j}^{\text{GES}}$  are cost coefficients of GES asset  $j$ .  $P_{d,j,t}^{\text{GES}}$ ,  $P_{c,j,t}^{\text{GES}}$  are the discharge and charge power of GES asset  $j$ .  $\Delta t$  is the unit dispatch interval.  $\lambda_t$  is the electricity price.  $P_t^{\text{grid}}$  is the power imported from the grid.  $P_{k,t}^{\text{DG}}$  is the power output of DG.  $a_k$  is cost coefficient of DG. Up and down ramp rate for  $P_{k,t}^{\text{DG}}$  are given by  $P_{k,\text{RU}}^{\text{DG}}$  and  $P_{k,\text{RD}}^{\text{DG}}$ . Underline and overline denote minimum and maximum.  $\varepsilon$  is the probability level of chance constraints.  $\mathcal{E}_j$ ,  $\eta_{c/d,j}$ ,  $E_j$  and  $\pi_{j,t}$  define the self-discharge rate, charge/discharge efficiency, capacity, and baseline consumption item.  $b$ ,  $m$  are the index of branches and buses,  $Br(m)$  is the set of branches that connect to bus  $m$ ,  $Br(m, l)$  is the set of the branch between bus  $m$  and  $l$ ,  $P_{b,t}^{\text{PF}}$ ,  $Q_{b,t}^{\text{PF}}$  are the active and reactive power that flows on branch  $b$ ,  $P_{b,0,t}^{\text{PF}}$ ,  $Q_{b,0,t}^{\text{PF}}$  are the active and reactive power that flows on the lateral branch. We set the GES to have a

fixed power factor.  $P_{m,t}^{\text{L}}$ ,  $P_{m,t}^{\text{R}}$  are the power of load and RES.  $V_{m,t}^{\text{BUS}}$  is the voltage of bus  $m$ ,  $V^{\text{B}}$  is voltage of the substation bus,  $R_b$ ,  $X_b$  is the resistance and reactance of branch  $b$ .

### III. DATA-DRIVEN TWO-STAGE COORDINATED DISPATCH OF MG BASED ON OCO

Solving the proposed offline dispatch model, although theoretically optimal, faces practical challenges due to two main reasons: (i) the uncertainties of the power and SoC limits of GES, which are both time-varying and stochastic. These uncertainties render the chance constraints (5) and (7) intractable; (ii) the model's inability to adapt to real-time changes such as price fluctuations and RES variabilities, can lead to poor economic performance and potential voltage violations.

To address these issues, this paper adopts a deterministic reformulation that makes the chance constraints tractable. We redefine MG dispatch as an online decision-making process that dynamically incorporates uncertainties as they are revealed during real-time operations. An adaptive VQB online optimization algorithm is developed, leveraging the latest uncertainty data for real-time control. To counteract the potential for myopic decision-making, which is often a consequence of the lack of prediction and the interconnected nature of GES operations, a two-stage coordinated dispatch approach is introduced as illustrated in Fig. 1.

#### A. Chance-Constrained Reformulation

Chance constraints (5) and (7) allow for a deterministic and tractable reformulation [3]. We employ the standard reformulation from [24], and yields:

$$P_{c,j,t}^{\text{GES}} \leq \mu_{\overline{P}_{c,j,t}^{\text{GES}}} - F_{\overline{P}_{c,j,t}^{\text{GES}}}^{-1}(1 - \varepsilon) \sigma_{\overline{P}_{c,j,t}^{\text{GES}}} \quad (14a)$$

$$P_{d,j,t}^{\text{GES}} \leq \mu_{\overline{P}_{d,j,t}^{\text{GES}}} - F_{\overline{P}_{d,j,t}^{\text{GES}}}^{-1}(1 - \varepsilon) \sigma_{\overline{P}_{d,j,t}^{\text{GES}}} \quad (14b)$$

$$\text{SoC}_{j,t} \leq \mu_{\overline{\text{SoC}}_{j,t}} - F_{\overline{\text{SoC}}_{j,t}}^{-1}(1 - \varepsilon) \sigma_{\overline{\text{SoC}}_{j,t}} \quad (14c)$$

$$\text{SoC}_{j,t} \geq \mu_{\underline{\text{SoC}}_{j,t}} - F_{\underline{\text{SoC}}_{j,t}}^{-1}(1 - \varepsilon) \sigma_{\underline{\text{SoC}}_{j,t}} \quad (14d)$$

where normalized inverse cumulative distribution function  $F^{-1}$  can be obtained by Monte Carlo sampling of any kind of distribution (e.g., normal distribution, beta distribution) [25].  $\mu$ ,  $\sigma$  are the mean and standard deviation of the distribution. Thus, the dispatch model becomes convex programming and can be efficiently solved by commercial solvers.

#### B. Offline Stage: Empirical Learning

Compared to predictions, historical data are much more accessible. These data serve as a foundational element for empirical learning, enabling us to extract valuable insights for dispatch operations. Specifically, a collection of historical scenarios of net load (calculated by subtracting the RES power from the total load power) and price is utilized, denoted by:

$$\{\ell_{t,s}, \lambda_{t,s}\}_{t=1}^T, s \in \{1, 2, \dots, S\}, \quad (15)$$

where  $\ell_t$  is net load,  $S$  is the number of historical scenarios. For each scenario, we solve the day-long optimal dispatch model:

$$\begin{aligned} & \min \text{objective function (1)} \\ & \text{s.t. constraints (2)-(4), (6), (8)-(14),} \end{aligned} \quad (16)$$

and get  $S$  offline optimal SoC:  $\text{SoC}_s = \{\text{SoC}_{t,s}\}_{t=1}^T$ .

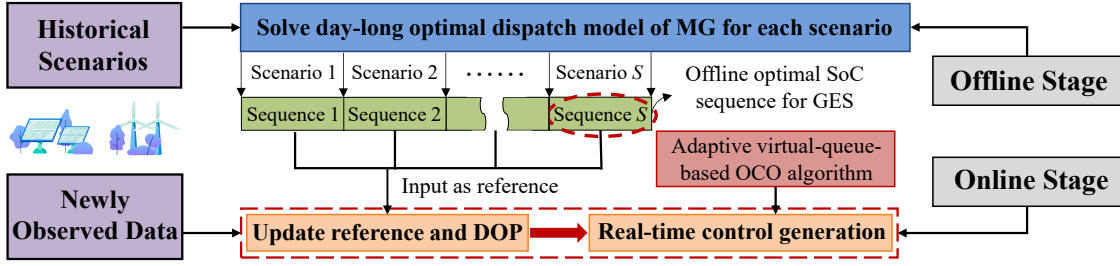


Fig. 1. Data-driven two-stage coordinated dispatch framework.

### C. Online Stage: Real-Time Control Policy

#### (a) Update reference

During the online stage of operation, real-time control actions are executed at five-minute intervals. Prior to these actions, the reference and the DOP are determined. The reference is crucial as it leverages historical data to mitigate the risk of myopic decision-making, thereby providing a broader perspective that aligns with long-term operational goals. The methodology for updating the reference is data-driven as it dynamically assigns weights to the offline optimal SoC sequences based on their relevance to the current scenario. Specifically, if the uncertainty realization observed during operation closely aligns with a particular historical scenario, that scenario's SoC sequence is given a larger weight coefficient in the reference calculation. This approach ensures that the reference is continually adjusted to reflect the most applicable historical insights.

Specifically, define vectors  $\ell_{[t]}$  and  $\lambda_{[t]}$  to represent the uncertainty observed in the real-time operation from the beginning of the operating day to the current period  $t$ :

$$\ell_{[t]} = [\ell_1, \dots, \ell_t], \lambda_{[t]} = [\lambda_1, \dots, \lambda_t]. \quad (17)$$

Define vectors that corresponds to the  $s$ th historical scenario:

$$\ell_{[t],s} = [\ell_{1,s}, \dots, \ell_{t,s}], \lambda_{[t],s} = [\lambda_{1,s}, \dots, \lambda_{t,s}]. \quad (18)$$

Consequently, the similarity between  $\ell_{[t]}$  and  $\ell_{[t],s}$  can be measured by the Euclidean distance as  $\|\ell_{[t]} - \ell_{[t],s}\|_2$ . Then, we can determine and sequentially update the reference by taking the weighted average of those offline optimal sequences. Let  $SoC_t^{\text{ref}}$  be the reference in period  $t$ , with the update policy defined as:

$$SoC_t^{\text{ref}} = \sum_{s=1}^S \omega_t^s SoC_{t,s}, \quad (19)$$

where  $\omega_t^s$  is the weight of historical scenario  $s$ , reflecting the similarity between the operating day and the  $s$ th historical scenario.  $\omega_t^s$  in period  $t$  is calculated using Nadaraya-Waston kernel regression technique [26]:

$$\omega_t^s = \frac{K_t(\ell_{[t]}, \ell_{[t],s}) K_t(\lambda_{[t]}, \lambda_{[t],s})}{\sum_{s'=1}^S [K_t(\ell_{[t]}, \ell_{[t],s'}) K_t(\lambda_{[t]}, \lambda_{[t],s'})]}, \quad (20)$$

where with  $x$  and  $y$  as the input vectors,

$$\text{where } K_t(x, y) = e^{-\frac{(\|x-y\|_2)^2}{t\tau}}. \quad (21)$$

is defined as the Gaussian kernel function;  $\tau$  is the bandwidth parameter. We have  $\sum_s \omega_t^s = 1$ , and scenarios more similar to the current day are assigned larger weight. Thus,  $\{\omega_t^s\}_{s=1}^S$

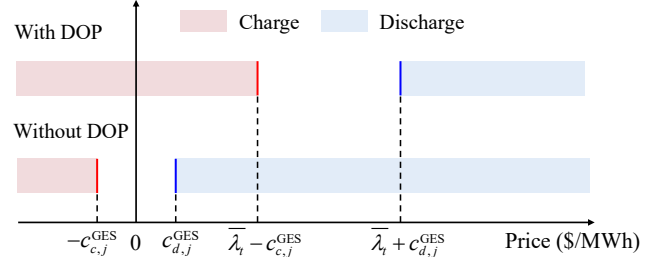


Fig. 2. Illustration of the impact of DOP on the GES actions.

can be viewed as a discrete probability distribution, and the reference can be viewed as the conditional expectation of  $S$  offline optimal sequences over the operating day. Utilizing the latest data, the reference is updated every 5 minutes, which is a sequential process along with time.

#### (b) Real-time control action generation—OCO algorithm

Following the update of the reference, real-time control actions are generated to minimize the instantaneous operating costs while adhering to the updated reference. Typically, the operational strategy would dictate that the GES discharges whenever it is economically beneficial, generally whenever prices are above  $c_{d,j}^{\text{GES}}$ , based on the SoC reference. This straightforward approach, while providing immediate benefits, is not necessarily optimal. A more strategic method involves discharging the GES when the prices are above the “average” and charging when the prices fall below the “average”. Consequently, we have made a revision to  $C_t^{\text{GES}}$ :

$$\hat{C}_t^{\text{GES}} = \sum_{j \in \Omega_G} ((c_{d,j}^{\text{GES}} + \bar{\lambda}_t) P_{d,j,t}^{\text{GES}} + (c_{c,j}^{\text{GES}} - \bar{\lambda}_t) P_{c,j,t}^{\text{GES}}) \Delta t, \quad (22)$$

with the update policy of  $\bar{\lambda}_t$  defined as:

$$\bar{\lambda}_t = \sum_{s=1}^S \omega_t^s \bar{\lambda}_{t,s}, \quad (23)$$

where  $\bar{\lambda}_t$  is the so-called DOP, and  $\bar{\lambda}_{t,s}$  is the average price for the  $s$ th scenario. Similarly, DOP can be viewed as the conditional expectation of the average price of the  $S$  scenarios over the operating day. Fig. 2 illustrates the impact of DOP on the charging and discharging trends of GES, enhancing the algorithm's ability to capitalize on peak-valley arbitrage opportunities. Therefore, the online decision optimization problem in period  $t$  can be formulated as (24a).

$$\begin{aligned} \min f_t &= \hat{C}_t^{\text{GES}} + C_t^{\text{grid}} + C_t^{\text{DG}} + \varphi (SoC_t - SoC_t^{\text{ref}})^2 \quad (24a) \\ \text{s.t.} & \text{ constraints (2)–(4), (6), (9)–(14)} \end{aligned}$$

$$\min_{x_t} f_t(x_t) \text{ s.t. } g_t(x_t) \leq 0, t = 1, 2, \dots, T \quad (24b)$$

---

**Algorithm 1** : Data-driven adaptive VQB OCO Algorithm
 

---

**[Offline Stage For Empirical Learning]**
**Input:** Historical scenarios of net load and price:

$$\{\ell_{t,s}, \lambda_{t,s}\}_{t=1}^T, s \in \{1, 2, \dots, S\}.$$

**For**  $s = 1, \dots, S$ 

Solve the day-long optimal model (16).

   Store the optimal SoC sequence  $SoC_s$ .

**end**
**[Online Stage For Real-Time Control]**
**Step 1 - Initialization:**

 Set  $Q_i(0) = 0$ ,  $x_{i,1} \in X$ ,  $x_1 = \sum_{i=1}^N \rho_{i,1} x_{i,1}$ ,

$$\rho_{i,1} = (N+1)/[i(i+1)N], \forall i \in \{1, 2, \dots, N\}.$$

**Step 2 - Iteration:**
**For**  $t = 2, \dots, T$ 

   Update reference  $SoC_t^{\text{ref}}$  and DOP using (19)-(21), (23).

   Update  $Q_i$  for each expert in parallel using (27).

   Update  $x_{i,t}$  for each expert in parallel using (26).

   Execute weighted average  $x_t$  calculated by (28).

   Observe  $f_t(x_t)$  and  $g_t(x_t)$ .

Update the weight of each expert by (29).

**end**
**Step 3 - Output:**  $x_t, f_t(x_t), t = 1, \dots, T$ , regret, violation.
 

---

The second part in the objective represents the penalty for deviation from the reference, where  $\varphi$  is weight coefficient. Constraint (8) is excluded, as (24a) is local optimization, unsuitable for addressing inter-temporal constraints. However, appropriately tracking the reference can still ensure a sustainable energy state for the GES overtime.

(24a) admits a compact form in (24b), which is the general problem formulation addressed by OCO.  $x_t$  refers to the discharge and charge power of GES, the power output of DG, and power curtailment of PV and WT. In the online operation, decisions are applied to the subsequent 5-minute interval. However, the uncertainties of RES and prices are only revealed after the decisions are made. This means that some constraints and the objective function in (24b) cannot be modeled accurately in real-time, i.e., decision is made before the observation of the uncertainty. Sequential decision-making problems under this “0-lookahead” pattern are typically addressed through OCO [8].

We have developed a novel adaptive VQB OCO algorithm tailored for effectively addressing the decision-making challenges outlined in problem (24b). The main theoretical advancements of our algorithm are encapsulated in Theorem 1, where we have proven the achievement of sublinear dynamic regret and sublinear strict constraint violation bounds—a first in the field of OCO. The algorithmic framework, detailed in Algorithm 1, integrates both the offline and online stages, including the critical updates to the reference and DOP. It is important to note that the inherent properties of our algorithm, as described in Theorem 1, are maintained regardless of these updates. To elucidate the underlying mechanics of our approach, we initiate our discussion with the application of the Lagrange multiplier method, setting the stage for a deeper

exploration of the algorithm’s operational dynamics, given as:

$$x_t = \operatorname{argmin}_{x \in X} L_t(\lambda_t, x) = \operatorname{argmin}_{x \in X} \{f_t(x) + \langle \lambda_t, g_t(x) \rangle\}, \quad (25)$$

where  $\lambda_t$  is the dual variables and  $\langle x, y \rangle$  denotes the standard inner product. In the online setting, we lack prior knowledge of  $f_t$  and  $g_t$  when making decision  $x_t$ . We estimate  $f_t$  using first-order Taylor expansion, and use the clipper constraint function  $[g_{t-1}(x)]_+$  to replace  $g_t(x)$ .  $\lambda_t$  is substituted by virtual queue  $Q(t-1)$  acting like a “queue backlog” of constraint violations. The regularization term  $\|x - x_{t-1}\|^2$  is added to smooth the difference between coherent actions and enhance the stability of the algorithm. With these adjustments, (25) can be transformed into its online counterpart:

$$x_t = \operatorname{argmin}_{x \in X} \{ \alpha_{t-1} \langle \partial f_{t-1}(x_{t-1}), x - x_{t-1} \rangle + \alpha_{t-1} \beta_{t-1} \langle Q(t-1), [g_{t-1}(x)]_+ \rangle + \|x - x_{t-1}\|^2 \}. \quad (26)$$

We update each element in the virtual queue with (27). The update strategy is that when violation occurs the violation is accumulated into virtual queue, and we use a round-dependent variable  $\theta_{t-1}$  to guarantee a minimum value of virtual queue that prevent the algorithm from taking aggressive decisions which lead to large constraint violation.

$$Q^k(t-1) = \max(Q^k(t-2) + \beta_{t-1} [g_{t-1}^k(x_{t-1})]_+, \theta_{t-1}) \quad (27)$$

Then, the most critical issue is to determine the learning rate  $\alpha_{t-1}$  for (26), one of the key parameters in optimization. A fixed learning rate may not adapt well to changes in the environment during online optimization. Inspired by [27], we use the expert tracking algorithm to address this dilemma. Our idea is to run multiple (26), i.e., experts, in parallel, each with a different learning rate  $\alpha_{t-1}$ , and then a set of actions  $x_{t-1}$  are generated by all experts, finally we output the weighted average as (28). After observing the objective function  $f_t$ , the weights of each expert  $\rho_{i,t}$  are updated according to their empirical performance on the data using an exponential weighting scheme, as shown in (29).

$$x_t = \sum_{i=1}^N \rho_{i,t} x_{i,t} \quad (28)$$

$$l_t(x_{i,t}) = \langle \partial f_t(x_t), x_{i,t} - x_t \rangle, \rho_{i,t+1} = \frac{\rho_{i,t} e^{-\gamma l_t(x_{i,t})}}{\sum_{i=1}^N \rho_{i,t} e^{-\gamma l_t(x_{i,t})}} \quad (29)$$

Based on the above analysis, we put forward Algorithm 1 and are ready to present the main result of the algorithm. First, we make the following assumptions on the objective function and constraint function, which are useful in later analysis. Notably, these assumptions align with standard practices in OCO literature and are applicable to the dispatch of MG.

*Assumption 1.* The function  $f_t$  and  $g_t$  are convex. The set  $X$  is convex and there is a positive constant  $d(X)$  such that

$$\|x - y\| \leq d(X), \forall x, y \in X. \quad (30)$$

*Assumption 2.* There exists a positive constant  $F$  such that

$$|f_t(x) - f_t(y)| \leq F, \|g_t(x)\| \leq F, \forall t, \forall x, y \in X. \quad (31)$$

*Assumption 3.* The subgradients  $\partial f_t(x)$  and  $\partial g_t(x)$  exist. There exists a positive constant  $G$  such that

$$\|\partial f_t(x)\| \leq G, \|\partial g_t(x)\| \leq G, \forall t, \forall x, y \in X. \quad (32)$$

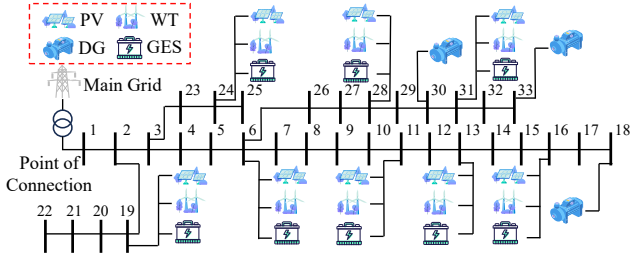


Fig. 3. 33-bus radial MG diagram.

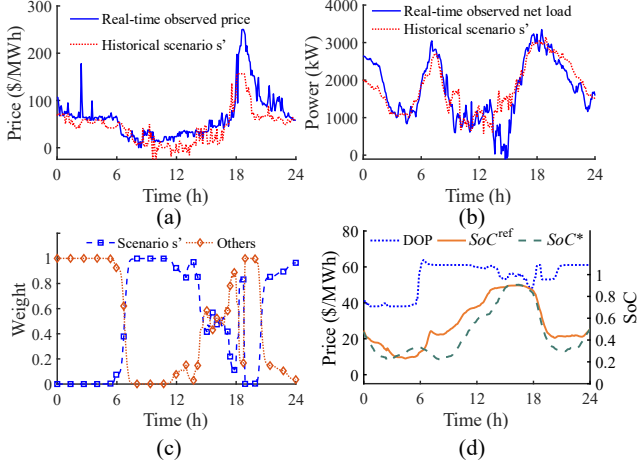


Fig. 4. (a) Prices, (b) Net load, (c) the weight variations of historical scenarios, and (d) the updating process of the reference and DOP for day 7.

The regret and strict constraint violation bounds for Algorithm 1 are provided in the following theorem.

**Theorem 1.** Suppose Assumption 1-3 hold. For any  $T \in \mathbb{N}_+$ , if we choose appropriate  $N$ ,  $\gamma$ ,  $\{\alpha_{i,t}\}$ ,  $\{\beta_t\}$  and  $\{\theta_t\}$ :

$$N = \left\lceil \frac{1}{2} \log_2(1+T) \right\rceil + 1, \quad \gamma = \frac{1}{\sqrt{T}}, \quad \alpha_{i,t} = \frac{2^{i-1}}{t^{\frac{1}{2} + \chi}}, \quad (33)$$

$$\beta_t = t^{\frac{1}{2} + \delta}, \quad \theta_{i,t} = 2^{i-1}t, \quad \forall i \in \{1, 2, \dots, N\}, \quad \frac{1}{2} > \delta > \chi > 0,$$

then Algorithm 1 achieves:

$$\text{regret} = \sum_{t=1}^T [f_t(x_t) - f_t(x_t^*)] = O(T^{\frac{1}{2} + \chi} \sqrt{1 + P_x}), \quad (34)$$

$$\text{Vio}^{\text{strict}} = \sum_{t=1}^T \|[g_t(x_t)]_+\| = O(\log_2(T) T^{1 - \frac{\chi}{2}}), \quad (35)$$

where  $\{x_t^*\}$  is the global optimal solution.  $P_x$  is defined as:

$$P_x = \sum_{t=1}^{T-1} \|x_{t+1}^* - x_t^*\|. \quad (36)$$

**Proof:** The proof is given in Appendix.

#### IV. CASE STUDY

##### A. Set-up

The proposed method is tested on the IEEE 33 bus radial system, which has been configured as a MG, illustrated in Fig. 3 [28]. This test system was populated with ground-truth data collected at 5-minute intervals, covering solar, wind, load, and price, all sourced from the Australian Energy Market

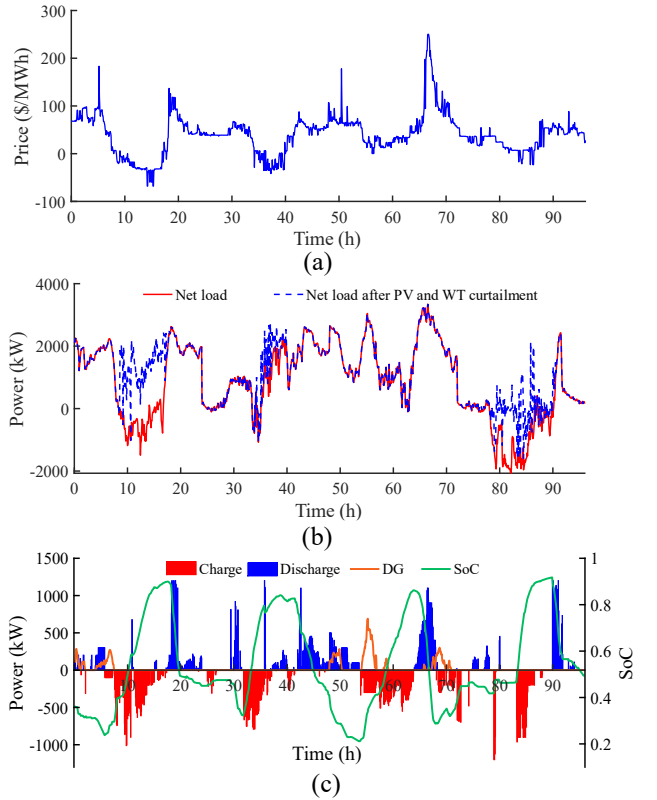


Fig. 5. (a) Prices, (b) net load, and (c) dispatch results for day 5-8.

Operator's publicly available datasets. The rated power of WT, PV, DG, ES, and VES are 2.5MW, 2.5MW, 1.5MW, 1.2MW, and 0.6MW, with an average load of approximately 2.5MW. The voltage at each bus is constrained to remain within  $1 \pm 0.05$  p. u. All related data, including time-varying SoC bounds for GES and detailed system configurations, are made publicly available [29]. We assume that the uncertainties (prices, RES, load) are revealed 5 minutes after the decision is made. The computational analyses were performed on a Core i7-1165G7 @ 2.80GHz, 16GB RAM laptop. The whole problem is coded in MATLAB equipped with the YALMIP interface and solved using CPLEX 12.6.

##### B. Dispatch Results Compared With Different Methods

We implemented the proposed method for a two-month dispatch, with results shown in Figs. 4-6. Taking day 7 as an example, Fig. 4 illustrates the dynamic updating process of the reference and DOP, where  $s'$  is the historical scenario most similar to day 7, and  $SoC^*$  represents the optimal SoC obtained by the deterministic method with perfect knowledge. As shown in Fig. 4, through (20), the weights of historical scenarios are continuously updated based on their similarity to the operating day and dynamically generate the reference SoC and DOP through (19) and (23). The trend of the reference SoC is similar to that of the optimal SoC; the DOP fluctuates around \$60/MWh, very close to the actual average price of \$65/MWh on day 7. The reference and DOP provide a global vision for online optimization.

Fig. 5 illustrates the dispatch results for days 5 to 8, where real-time control actions generated by the OCO algorithm effectively minimized operating costs while adhering to voltage constraints. The GES dynamically discharges when

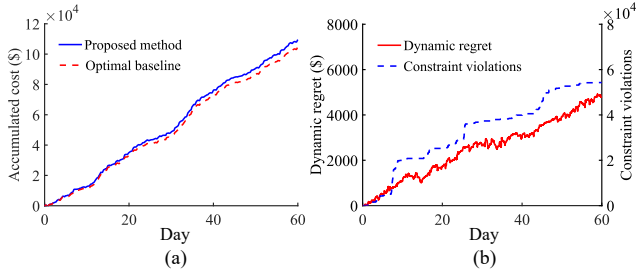


Fig. 6. (a) Accumulated cost, (b) regret and violations over 2 months.

prices exceed  $\bar{\lambda}_t + c_{d,j}^{\text{GES}}$  and charges when prices fall below  $\bar{\lambda}_t - c_{c,j}^{\text{GES}}$ . Additionally, curtailment of WT and PV power is implemented during periods of negative pricing. As shown in Fig. 6, the accumulated cost over the two-month period deviated by only 4.57% from the optimal baseline, demonstrating the effectiveness of the proposed method. Moreover, the growth in dynamic regret and constraint violations primarily resulting from constraints (12) and (13) followed largely sublinear trends, aligning with the theoretical predictions established in Theorem 1. Voltage levels throughout the operation predominantly stayed within safe limits, maintaining a voltage satisfaction rate of 98.24%.

To contextualize the performance of our method, we conducted comparisons with several alternative approaches:

- 1) **M0**: Deterministic optimization with perfect knowledge. This method is impractical and serves as an optimal baseline.
- 2) **M1**: The proposed prediction-free coordinated approach.
- 3) **M2**: Economic MPC [4], to the authors' best knowledge, is currently the state-of-the-art method. Adopting the scheduling-correction framework proposed in [30], reference is generated and MPC is utilized for online optimization. Short-term prediction of net load and prices is generated with prediction error (MAPE) set as 10% and 20%, respectively.
- 4) **M3**: The online dispatch approach for MG based on Lyapunov optimization proposed in [9].

The dispatch outcomes of M0-M3 over a two-month period are detailed in Table II. M2\* is MPC method with MAPE set at 15% and 30%, respectively. As indicated in Fig. 7, SoC of M3 deviates most significantly from the optimal baseline. This larger deviation is attributed to the inherently myopic nature of the Lyapunov optimization, which, as a purely online process, focuses on minimizing immediate operational costs. Typically, it tends to discharge during positive prices and charge during negative ones, resulting in the SoC predominantly remaining below 0.5. The rationale behind charging during positive price periods is to maintain stability within the “battery queue.” This approach aims to manage the queue backlogs more effectively, achieving smaller average backlogs. However, these operational decisions are clearly myopic and lead to substantially

TABLE II  
COMPARISONS OF OPERATIONAL PERFORMANCE OVER 2 MONTHS

Indices	M0	M1	M2	M2*	M3
Operation cost (\$)	104762	109548	115347	124039	122980
Voltage satisfaction rate (%)	100	98.27	89.49	87.33	98.15
Computation time (min/day)	/	1.9	37.6	37.6	1.9

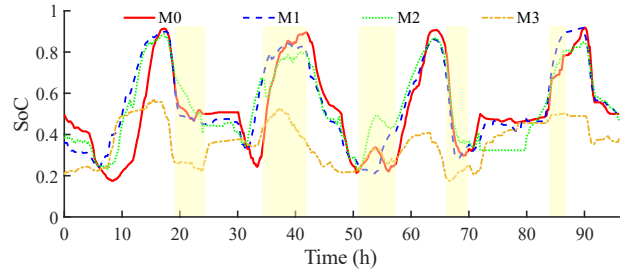


Fig. 7. Comparison of SoC between M0-M3 for day 5-8.

higher operational costs in the long run, demonstrating the limitations of relying solely on immediate pricing signals without a strategic, long-term perspective on GES operation.

The SOC of M2 generally resembles those of M1 and M0. However, if the forecasts or references are inaccurate, inferior decisions may be made (Fig. 7 19-24h, 34-41h, 50-56h, 66-69h, 83-86h). In contrast, M1 can quickly respond to the change of RES and prices based on newly observed data, and continuously adapts learning rate according to (29). Moreover, M1 considers DOP, which allows for some performance sacrifices occasionally but achieves better overall performance in the end. For example, during the 19th hour, there was an unexpected surge in prices, to which M2 could not respond promptly. Based on real-time observed data, M1 significantly increased the discharge power, thereby reducing operational costs. Similarly, during the 85th hour, when negative price spikes occurred frequently, M1 was able to respond and track these rapid changes. It is evident that its charging power was significantly higher than that of M2, which also led to reduced operational costs. During hours 64-68, as the net load power rose rapidly and peaked, M1 effectively prevented voltage violations by increasing the discharge power. In contrast, M2 performed less effectively; the unbalanced power was absorbed by the external grid, causing excessively low voltage at the node far from the point of common coupling, as shown in Fig. 8. Additionally, a drawback of the MPC-based method is that its operational performance deteriorates with increasing prediction errors, as shown in Table II. In summary, M1 demonstrates better adaptability to time-varying environments.

In terms of computation time, M1 calculates much faster than M2. The core step of OCO, (26), only needs to solve an approximately unconstrained optimization problem, which is highly efficient. In contrast, the predictive and optimization model of MPC contains the system states over a certain future time interval, which makes the model much larger. Therefore, M1 is more suitable for online operation compared to M2.

### C. Discussion

#### (a) Benefit from reference

To demonstrate the benefit from data-driven coordinated dispatch, we compare the results for the following variants of M1:

1) **M1-a**: GES is dispatched strictly according to the reference, that is, the value of  $\varphi$  in (24a) is very large.

2) **M1-b**: online optimization without the reference.

The dispatch results are compared in Table III. Due to the non-anticipativity of RES and prices, references do not always approximate the optimal baseline. For instance, when prices suddenly increase (Fig. 9 67-71h), it is necessary for GES

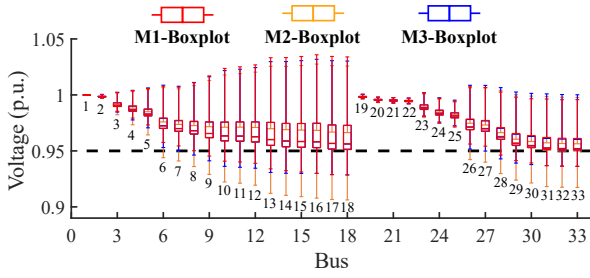


Fig. 8. Comparison of voltage distribution between M0-M3 for day 5-8.

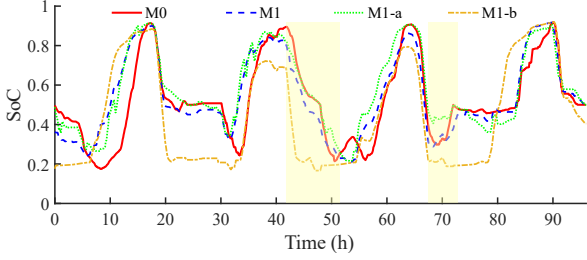


Fig. 9. Comparison of SoC between different variants of M1 for day 5-8.

to discharge promptly to reduce purchasing costs, rather than strictly following the reference. Thus, M1-a fails to adapt to the real-time changes of uncertainties, resulting in increased costs. Without a reference, however, the dispatch of GES tends to lack foresight. As shown in Fig. 9, M1-b consistently tends to “charge and discharge aggressively,” leaving not enough reserve for future dispatch. For example, during 41-43h, SoC dropped to its minimum. Then, during 47-51h, when the prices increased unexpectedly, GES lacked sufficient capacity to discharge. So we need to properly follow the reference. We have the weight parameter  $\varphi$  in (24) to control how close we expect the actual SoC of GES to be to the reference. Fig. 10 gives the sensitivity analysis of  $\varphi$ . The cost first goes up and then goes down with  $\varphi$  increasing. An interesting observation is that strictly following the reference yields worse performance than having no reference at all, which fully demonstrates the importance of online correction based on OCO.

#### (b) Benefit from DOP

To demonstrate the benefit from DOP, we compare the results between M1 and M1-c.

**M1-c:** Two-stage coordinated dispatch without considering DOP, that is,  $\hat{C}_t^{\text{GES}}$  in (24a) is replaced by  $C_t^{\text{GES}}$ .

As shown in Fig. 11, the SoC of M1-c is consistently lower than that of M1. This is because, without considering DOP, GES tends to discharge based on the reference when prices are above  $c_{d,j}^{\text{GES}}$ , as discharging reduces the immediate operational costs. DOP effectively estimates the average prices for a future period. In contrast, M1 tends to discharge when prices are higher than  $\bar{\lambda}_t + c_{d,j}^{\text{GES}}$  and charge when prices are lower than  $\bar{\lambda}_t - c_{c,j}^{\text{GES}}$ . This strategy effectively capitalizes on peak-valley arbitrage, and by appropriately sacrificing immediate benefits, it results in lower operational costs in the long term.

TABLE III  
COMPARISONS BETWEEN DIFFERENT VARIANTS OF M1 OVER 2 MONTHS

Indices	M1	M1-a	M1-b	M1-c
operation cost (\$)	109548	137849	117008	113842

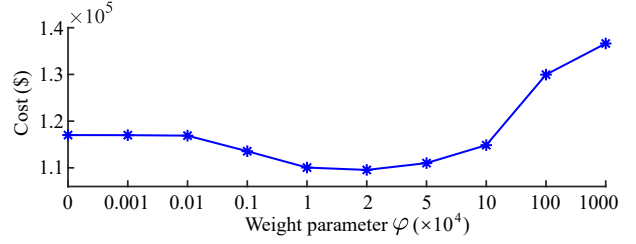


Fig. 10. Operation cost achieved by M1 with different  $\varphi$ .

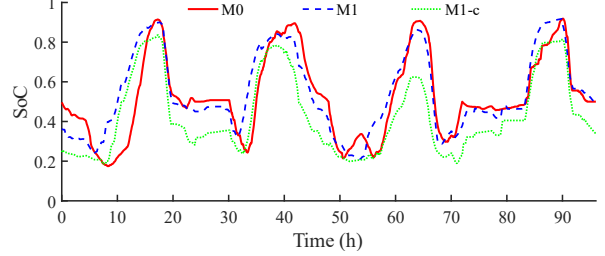


Fig. 11. Comparison of SoC between M1 and M1-c.

## V. CONCLUSION

This paper proposes a prediction-free coordinated dispatch framework for MG, designed to address the inherent myopia of online optimization. Central to this framework is an innovative adaptive VQB online optimization algorithm developed within the OCO framework. Simulation results verify that:

(1) The proposed method outperforms existing online optimization approaches. Compared with MPC-based method that relies on high-accuracy forecast data and Lyapunov optimization, it reduces operational costs by 5% and 11%, respectively. Additionally, the optimality gap is only 4.57% compared to deterministic methods with perfect foresight of uncertainties.

(2) The incorporation of a “reference” within the dispatch provides a global vision, crucial for avoiding myopic decisions during real-time operation. The weight parameter  $\varphi$  should be moderately set, so that the actual SoC can properly follow the reference and enhance overall operational performance.

(3) Incorporating DOP within OCO can reduce costs in the long run by continually adjusting to mirror the actual average price. It enhances the ability to capitalize on peak-valley arbitrage opportunities. OCO utilizes newly observed data for on-line correction, ensuring the safe operation of MG, evidenced by a 98.27% voltage satisfaction rate. Additionally, the computational speed makes it fully suitable for online applications.

Future work will explore the application of OCO to distributed optimization in power systems, real-time electricity trading, and online dispatch for networks of multiple MGs.

## APPENDIX

### A. Proof of the bound on dynamic regret

Let  $\{x_{i,t}\} (\forall i \in \{1, 2, \dots, N\})$  and  $\{x_t\}$  be the sequence generated by Algorithm1. Let  $\{y_t\}$  be an arbitrary sequence in  $X$ . From  $f_t$  is convex and (32), we have

$$\begin{aligned}
 f_t(x_{i,t}) - f_t(y_t) &\leq \langle \partial f_t(x_{i,t}), x_{i,t} - y_t \rangle \\
 &\leq G \|x_{i,t} - x_{i,t+1}\| + \langle \partial f_t(x_{i,t}), x_{i,t+1} - y_t \rangle \\
 &\leq \frac{G^2 \alpha_{i,t}}{2} + \frac{1}{2\alpha_{i,t}} \|x_{i,t} - x_{i,t+1}\|^2 + \langle \partial f_t(x_{i,t}), x_{i,t+1} - y_t \rangle
 \end{aligned} \tag{37}$$



For the third term of (37), we have

$$\begin{aligned} & \langle \partial f_t(x_{i,t}), x_{i,t+1} - y_t \rangle \\ &= \langle \beta_{t+1}(Q_i(t) \circ \partial[g_t(x_{i,t+1})]_+), y_t - x_{i,t+1} \rangle \\ &+ \langle \partial f_t(x_{i,t}) + \beta_{t+1}(Q_i(t) \circ \partial[g_t(x_{i,t+1})]_+), x_{i,t+1} - y_t \rangle. \end{aligned} \quad (38)$$

It is trivial that  $[g_t]_+$  is convex. We have

$$\begin{aligned} & \langle \beta_{t+1}(Q_i(t) \circ \partial[g_t(x_{i,t+1})]_+), y_t - x_{i,t+1} \rangle \\ & \leq \beta_{t+1} \langle Q_i(t), [g_t(x_{i,t+1})]_+ \rangle. \end{aligned} \quad (39)$$

Note that (26) can be written in the following form:

$$x_{i,t+1} = \operatorname{argmin}_{x \in X} \{h(x) + \|x - x_{i,t}\|^2\}. \quad (40)$$

From Lemma 1 in reference [31], we have:

$$\begin{aligned} & \langle \partial f_t(x_{i,t}) + \beta_{t+1}(Q_i(t) \circ \partial[g_t(x_{i,t+1})]_+), x_{i,t+1} - y_t \rangle \\ & \leq \frac{1}{\alpha_{i,t}} (\|y_t - x_{i,t}\|^2 - \|y_t - x_{i,t+1}\|^2 - \|x_{i,t+1} - x_{i,t}\|^2). \end{aligned} \quad (41)$$

Combining (37), (38), (39) and (41) gives

$$\begin{aligned} f_t(x_{i,t}) - f_t(y_t) & \leq \frac{G^2 \alpha_{i,t}}{2} + \frac{1}{\alpha} (\|y_t - x_{i,t}\|^2 - \|y_t - x_{i,t+1}\|^2) \\ & + \beta_{t+1} \langle Q_i(t), [g_t(y_t)]_+ \rangle. \end{aligned} \quad (42)$$

Let the optimal sequence be  $\{x_t^*\}$ . Substitute  $\{y_t\} = \{x_t^*\}$  in (42). Note that  $g_t(x_t^*) \leq 0$  because  $\mathcal{X}_t^* \in X$ , which gives

$$\begin{aligned} & \sum_{t=1}^T f_t(x_{i,t}) - \sum_{t=1}^T f_t(x_t^*) \\ & \leq \sum_{t=1}^T \frac{1}{\alpha_{i,t}} (\|x_t^* - x_{i,t}\|^2 - \|x_t^* - x_{i,t+1}\|^2) + \sum_{t=1}^T \frac{G^2 \alpha_{i,t}}{2}. \end{aligned} \quad (43)$$

Using (30) and (33) yields

$$\begin{aligned} & \sum_{t=1}^T \frac{1}{\alpha_{i,t}} (\|x_t^* - x_{i,t}\|^2 - \|x_t^* - x_{i,t+1}\|^2) \\ & \leq \frac{1}{2^{i-1}} ((d(X))^2 (T+1)^{\frac{1}{2}+\chi} + 2d(X)P_x T^{\frac{1}{2}+\chi}). \end{aligned} \quad (44)$$

For the second term of (43), we have

$$\sum_{t=1}^T \frac{G^2 \alpha_{i,t}}{2} \leq \frac{2^{i-1} G^2}{2} \sum_{t=1}^T \frac{1}{t^{\frac{1}{2}+\chi}} \leq \frac{2^{i-1} G^2}{1-2\chi} T^{\frac{1}{2}-\chi}. \quad (45)$$

Combining (43)-(45) gives

$$\begin{aligned} \sum_{t=1}^T f_t(x_{i,t}) - \sum_{t=1}^T f_t(x_t^*) & \leq \frac{2}{2^{i-1}} ((d(X))^2 T^{\frac{1}{2}+\chi} (1 + \frac{P_x}{d(X)})) \\ & + \frac{2^{i-1} G^2}{1-2\chi} T^{\frac{1}{2}-\chi}. \end{aligned} \quad (46)$$

Let  $i_0 = \left\lceil \frac{1}{2} \log_2(1 + \frac{P_x}{d(X)}) \right\rceil + 1 \in [N]$  such that

$$2^{i_0-1} \leq \sqrt{1 + \frac{P_x}{d(X)}} \leq 2^{i_0}. \quad (47)$$

Substitute  $i_0$  in (46), and combining (46) and (47) yield

$$\sum_{t=1}^T f_t(x_{i_0,t}) - \sum_{t=1}^T f_t(x_t^*) \leq (4(d(X))^2 + \frac{G^2}{1-2\chi}) T^{\frac{1}{2}+\chi} \sqrt{1 + \frac{P_x}{d(X)}}. \quad (48)$$

From (29) and that  $f_t$  is convex, we have

$$f_t(x_t) - f_t(x_{i_0,t}) \leq l_t(x_t) - l_t(x_{i_0,t}). \quad (49)$$

Applying Lemma 1 in reference [27] to (28) and (29) yields

$$\sum_{t=1}^T l_t(x_t) - \min_{i \in [N]} \left\{ \sum_{t=1}^T l_t(x_{i,t}) + \frac{1}{\gamma} \ln \frac{1}{\rho_{i,1}} \right\} \leq \frac{\gamma (Gd(X))^2 T}{2}. \quad (50)$$

$$\sum_{t=1}^T f_t(x_t) - \sum_{t=1}^T f_t(x_{i_0,t}) \leq \frac{(Gd(X))^2 \sqrt{T}}{2} + \sqrt{T} \ln \frac{1}{\rho_{i_0,1}}. \quad (51)$$

From  $\rho_{i,1} = (N+1)/[i(i+1)N]$ , we have

$$\ln \frac{1}{\rho_{i_0,1}} \leq \ln(i_0(i_0+1)) \leq 2\ln(i_0+1) \leq 2\ln\left(\left[\frac{1}{2} \log_2(1 + \frac{P_x}{d(X)})\right] + 1\right) \quad (52)$$

Combining (48), (51) and (52) yields (34).

## B. Proof of the bound on cumulative constraint violations

Define

$$\begin{aligned} p_t(x) & := \alpha_{i,t} \langle \partial f_t(x_{i,t}), x - x_{i,t} \rangle \\ & + \alpha_{i,t} \beta_t \langle Q_i(t), [g_t(x)]_+ \rangle + \|x - x_{i,t}\|^2. \end{aligned} \quad (53)$$

Note that  $p_t(x)$  and  $\|x - x_t\|^2$  are 2-strongly convex, which gives

$$p(x) \geq p(y) + \langle \partial p(y), x - y \rangle + \|x - y\|^2. \quad (54)$$

According to (26), we have  $x_{i,t+1} = \operatorname{argmin}_{x \in X} p(x)$ . Based on the first-order optimality condition, we have

$$\langle \partial p(x_{i,t+1}), x - x_{i,t+1} \rangle \geq 0. \quad (55)$$

Substitute  $y = x_{i,t+1}$  and  $x = x_t^*$  in (54), and combining (53)-(55) yields

$$\begin{aligned} & \alpha_{i,t} \langle \partial f_t(x_{i,t}), x_{i,t+1} - x_{i,t} \rangle + \alpha_{i,t} \beta_t \langle Q_i(t), [g_t(x_{i,t+1})]_+ \rangle \\ & + \|x_{i,t+1} - x_{i,t}\|^2 \\ & \leq \alpha_{i,t} \langle \partial f_t(x_{i,t}), x_t^* - x_{i,t} \rangle + \alpha_{i,t} \beta_t \langle Q_i(t), [g_t(x_t^*)]_+ \rangle \\ & + \|x_t^* - x_{i,t}\|^2 - \|x_t^* - x_{i,t+1}\|^2. \end{aligned} \quad (56)$$

We add  $\alpha_{i,t} f_t(x_{i,t})$  to both sides and rearranging terms:

$$\begin{aligned} & \alpha_{i,t} f_t(x_{i,t}) - \alpha_{i,t} (f_t(x_{i,t}) + \langle \partial f_t(x_{i,t}), x_t^* - x_{i,t} \rangle) \\ & + \alpha_{i,t} \beta_t \langle Q_i(t), [g_t(x_{i,t+1})]_+ \rangle \\ & \leq \alpha_{i,t} \langle \partial f_t(x_{i,t}), x_{i,t} - x_{i,t+1} \rangle + \alpha_{i,t} \beta_t \langle Q_i(t), [g_t(x_t^*)]_+ \rangle \\ & - \|x_{i,t+1} - x_{i,t}\|^2 + \|x_t^* - x_{i,t}\|^2 - \|x_t^* - x_{i,t+1}\|^2. \end{aligned} \quad (57)$$

From  $[g_t(x_t^*)]_+ = 0$ , combining (32) and (57) yields

$$\begin{aligned} & \alpha_{i,t} f_t(x_{i,t}) - \alpha_{i,t} f_t(x_t^*) + \alpha_{i,t} \beta_t \langle Q_i(t), [g_t(x_{i,t+1})]_+ \rangle \\ & \leq \frac{\alpha_{i,t}^2 G^2}{4} + \|x_t^* - x_{i,t}\|^2 - \|x_t^* - x_{i,t+1}\|^2. \end{aligned} \quad (58)$$

From (58), we have

$$\begin{aligned} & \alpha_{i,t}\beta_t\langle Q_i(t), [g_t(x_{i,t+1})]_+ \rangle \\ & \leq \frac{\alpha_{i,t}^2 G^2}{4} + \alpha_{i,t} |f_t(x_{i,t}) - f_t(x_t^*)| + \|x_t^* - x_{i,t}\|^2 - \|x_t^* - x_{i,t+1}\|^2. \end{aligned} \quad (59)$$

From (27), we have

$$\alpha_{i,t}\beta_t\langle Q_i(t), [g_t(x_{i,t+1})]_+ \rangle \geq \alpha_{i,t}\beta_t\theta_{i,t} \| [g_t(x_{i,t+1})]_+ \|_1. \quad (60)$$

Combining (33), (59) and (60) yields

$$\begin{aligned} \| [g_t(x_{i,t+1})]_+ \|_1 & \leq \frac{G^2}{4t^{2+\delta+\chi}} + \frac{|f_t(x_{i,t}) - f_t(x_t^*)|}{2^{i-1}t^{\frac{3}{2}+\delta}} \\ & \quad + \frac{\|x_t^* - x_{i,t}\|^2 - \|x_t^* - x_{i,t+1}\|^2}{4^{i-1}t^{1+\delta-\chi}}. \end{aligned} \quad (61)$$

Under Assumptions 1-3, summing (61) over  $t \in \{1, \dots, T\}$  yields

$$\sum_{t=1}^T \| [g(x_{i,t+1})]_+ \| \leq \frac{G^2}{2} + \frac{3F}{2^{i-1}} + \left(1 + \frac{1}{\delta-\chi}\right) \frac{(d(X))^2}{4^{i-1}}. \quad (62)$$

From Cauchy-Schwarz inequality, we have

$$\begin{aligned} & \| [g_t(x_{i,t})]_+ \|_1 - \| [g_t(x_{i,t+1})]_+ \|_1 \\ & \leq \| \partial [g_t(x_{i,t})]_+ \| \| \| x_{i,t} - x_{i,t+1} \| \leq \frac{G^2}{4\eta} + \eta \| x_{i,t} - x_{i,t+1} \|^2, \end{aligned} \quad (63)$$

where  $\eta = T^{\chi/2}$ . Summing (63) over  $t \in \{1, \dots, T\}$  yields

$$\begin{aligned} & \sum_{t=1}^T \| [g_t(x_{i,t})]_+ \|_1 - \| [g_t(x_{i,t+1})]_+ \|_1 \\ & \leq \frac{G^2}{4} T^{1-\frac{\chi}{2}} + 2^{i-1}(F+Gd(X)) \frac{2}{1-2\chi} T^{\frac{1}{2}-\frac{\chi}{2}} + (d(X))^2 T^{\frac{\chi}{2}} \end{aligned} \quad (64)$$

Combining (62) and (64) yields

$$\begin{aligned} & \sum_{t=1}^T \| [g_t(x_{i,t})]_+ \| \leq \frac{G^2}{2} + 3\frac{F}{2^{i-1}} + \left(1 + \frac{1}{\delta-\chi}\right) \frac{(d(X))^2}{4^{i-1}} \\ & \quad + (d(X))^2 T^{\frac{\chi}{2}} + \left(\frac{G^2}{4} T^{1-\frac{\chi}{2}} + 2^{i-1}(F+Gd(X))\right) \frac{2}{1-2\chi} T^{\frac{1}{2}-\frac{\chi}{2}} \end{aligned} \quad (65)$$

Combining (28), (29), (33) and (65) yields (35).

## REFERENCES

- [1] H. Qiu, W. Gu, X. Xu *et al.*, "A historical-correlation-driven robust optimization approach for microgrid dispatch," *IEEE Trans. Smart Grid*, vol. 12, no. 2, pp. 1135–1148, 2021.
- [2] K. Antoniadou-Plytaria, D. Steen, O. Carlson *et al.*, "Scenario-based stochastic optimization for energy and flexibility dispatch of a micro-grid," *IEEE Trans. Smart Grid*, vol. 13, no. 5, pp. 3328–3341, 2022.
- [3] N. Qi, P. Pinson, M. R. Almassalkhi *et al.*, "Chance-constrained generic energy storage operations under decision-dependent uncertainty," *IEEE Trans. Sustain. Energy*, 2023.
- [4] J. Hu, Y. Shan, Y. Yang *et al.*, "Economic model predictive control for microgrid optimization: A review," *IEEE Trans. Smart Grid*, 2023.
- [5] Z. Li, L. Wu, Y. Xu *et al.*, "Multi-stage real-time operation of a multi-energy microgrid with electrical and thermal energy storage assets: A data-driven mpc-adp approach," *IEEE Trans. Smart Grid*, vol. 13, no. 1, pp. 213–226, 2021.
- [6] C. Hu, Z. Cai, Y. Zhang *et al.*, "A soft actor-critic deep reinforcement learning method for multi-timescale coordinated operation of microgrids," *Prot. Control Mod. Power Syst.*, vol. 7, no. 1, p. 29, 2022.
- [7] M. Zhang, Z. Zhen, N. Liu *et al.*, "Optimal graph structure based short-term solar pv power forecasting method considering surrounding spatio-temporal correlations," *IEEE Trans. Ind. Appl.*, vol. 59, no. 1, pp. 345–357, 2022.
- [8] Z. Wang, W. Wei, J. Z. F. Pang *et al.*, "Online optimization in power systems with high penetration of renewable generation: Advances and prospects," *IEEE/CAA J. Autom. Sinica*, vol. 10, no. 4, pp. 839–858, 2023.
- [9] W. Shi, N. Li, C.-C. Chu *et al.*, "Real-time energy management in microgrids," *IEEE Transactions on Smart Grid*, vol. 8, no. 1, pp. 228–238, 2017.
- [10] X. Ding, L. Chen, P. Zhou *et al.*, "Dynamic online convex optimization with long-term constraints via virtual queue," *Inf. Sci.*, vol. 577, pp. 140–161, 2021.
- [11] H. Yu and M. J. Neely, "A low complexity algorithm with  $o(\sqrt{T})$  regret and  $o(1)$  constraint violations for online convex optimization with long term constraints," *J. Mach. Learn. Res.*, vol. 21, no. 1, pp. 1–24, 2020.
- [12] Q. Liu, W. Wu, L. Huang *et al.*, "Simultaneously achieving sublinear regret and constraint violations for online convex optimization with time-varying constraints," *Perform. Evaluation Rev.*, vol. 49, no. 3, pp. 4–5, 2022.
- [13] X. Yi, X. Li, T. Yang *et al.*, "Regret and cumulative constraint violation analysis for online convex optimization with long term constraints," in *Proc. Int. Conf. Mach. Learn.* PMLR, 2021, pp. 11998–12008.
- [14] X. Cao, J. Zhang, and H. V. Poor, "Constrained online convex optimization with feedback delays," *IEEE Trans. Autom. Control*, vol. 66, no. 11, pp. 5049–5064, 2021.
- [15] D. Muthirayan, J. Yuan, and P. P. Khargonekar, "Online convex optimization with long-term constraints for predictable sequences," *IEEE Control Syst. Lett.*, vol. 7, pp. 979–984, 2023.
- [16] X. Yi, X. Li, T. Yang *et al.*, "Regret and cumulative constraint violation analysis for distributed online constrained convex optimization," *IEEE Trans. Autom. Control*, 2022.
- [17] S.-J. Kim and G. B. Giannakis, "An online convex optimization approach to real-time energy pricing for demand response," *IEEE Trans. Smart Grid*, vol. 8, no. 6, pp. 2784–2793, 2017.
- [18] T. Zhao, A. Parisio, and J. V. Milanović, "Distributed control of battery energy storage systems for improved frequency regulation," *IEEE Trans. Power Syst.*, vol. 35, no. 5, pp. 3729–3738, 2020.
- [19] A. Lesage-Landry, H. Wang, I. Shames *et al.*, "Online convex optimization of multi-energy building-to-grid ancillary services," *IEEE Trans. Control Syst. Technol.*, vol. 28, no. 6, pp. 2416–2431, 2020.
- [20] Z. Li, Q. Guo, H. Sun *et al.*, "Sufficient conditions for exact relaxation of complementarity constraints for storage-concerned economic dispatch," *IEEE Trans. Power Syst.*, vol. 31, no. 2, pp. 1653–1654, 2016.
- [21] N. Qi, L. Cheng, H. Xu *et al.*, "Smart meter data-driven evaluation of operational demand response potential of residential air conditioning loads," *Appl. Energy*, vol. 279, p. 115708, 2020.
- [22] K. Baker and A. Bernstein, "Joint chance constraints in ac optimal power flow: Improving bounds through learning," *IEEE Trans. Smart Grid*, vol. 10, no. 6, pp. 6376–6385, 2019.
- [23] Z. Li and Y. Xu, "Temporally-coordinated optimal operation of a multi-energy microgrid under diverse uncertainties," *Appl. Energy*, vol. 240, pp. 719–729, 2019.
- [24] M. Vrakopoulou, B. Li, and J. L. Mathieu, "Chance constrained reserve scheduling using uncertain controllable loads part i: Formulation and scenario-based analysis," *IEEE Trans. Smart Grid*, vol. 10, no. 2, pp. 1608–1617, 2019.
- [25] T. Homem-de Mello and G. Bayraksan, "Monte carlo sampling-based methods for stochastic optimization," *Surveys in Operations Research and Management Science*, vol. 19, no. 1, pp. 56–85, 2014.
- [26] H. J. Bierens, "The nadaraya-watson kernel regression function estimator," 1988.
- [27] L. Zhang, S. Lu, and Z.-H. Zhou, "Adaptive online learning in dynamic environments," *Proc. Adv. Neural Inf. Process. Syst.*, vol. 31, 2018.
- [28] Z. Wang, B. Chen, J. Wang *et al.*, "Robust optimization based optimal dg placement in microgrids," *IEEE Trans. Smart Grid*, vol. 5, no. 5, pp. 2173–2182, 2014.
- [29] K. Huang, "Supporting data and system configuration," 2024. [Online]. Available: <https://data.mendeley.com/datasets/8j2zdf6h5j/2>
- [30] Z. Guo, W. Wei, J. Bai *et al.*, "Long-term operation of isolated microgrids with renewables and hybrid seasonal-battery storage," *Applied Energy*, vol. 349, p. 121628, 2023.
- [31] X. Yi, X. Li, L. Xie *et al.*, "Distributed online convex optimization with time-varying coupled inequality constraints," *IEEE Trans. Signal Process.*, vol. 68, pp. 731–746, 2020.